International Journal of Pure and Applied Mathematics
Volume 111 No. 2 2016, 319-330
ISSN: 1311-8080 (printed version); ISSN: 1314-3395 (on-line version)
url: http://www.ijpam.eu
doi: 10.12732/ijpam.v111i2.15

ijpam.eu

NUMERICAL MODELING OF RESIDUAL THERMAL STRESS IN Si_3N_4 BASED HIGH-POROUS COMPOSITE CERAMICS

Lev N. Rabinskiy[1 §], Pavel O. Poliakov[2],
Yury O. Soliayev[3], Sergey A. Sitnikov[4],
Ekaterina L. Kuznetsova[5]
[1,2,3,4,5]Moscow Aviation Institute
National Research University
125993, Volokolamsk Highway 4, Moscow, RUSSIAN FEDERATION

Abstract: Modeling of residual thermal stresses arising in silicon nitride-based porous fibrous ceramic materials with reinforcing dispersed inclusions was carried out. Calculations were made within quasi-static linear thermoelasticity on the presumption that the initial state at which there are no internal stresses in the media is realized during synthesis of the material at temperature of $1450^{\circ}C$. Modeling was carried out on three-dimensional representative fragments of fibrous structures generated using random algorithms with preset parameters of the materials' microstructure. Influence of the volume fraction and the size of the fillers in the form of spherical inclusions of silicon carbide on the residual thermal stresses realized within the structure of fibrous porous material is analyzed. It is demonstrated that the level of arising residual stresses can be comparable and, indeed, may exceed the fracture strength of considered porous materials.

AMS Subject Classification: 82DXX, 97M10
Key Words: modeling, residual stress, silicon nitride, thermoelasticity, fibrous structure, porosity, composite, fibrous high-porous matrix

1. Introduction

Silicon nitride-based ceramic has excellent mechanical, thermal-physical and dielectric properties. Silicon nitride-based products are widely used in various

Received: October 15, 2016
Revised: November 11, 2016
Published: December 11, 2016

© 2016 Academic Publications, Ltd.
url: www.acadpubl.eu

§Correspondence author

fields of technology [1] and [2], particularly, in assembly parts of jet engines, in fuel systems, braking systems elements. Silicon nitride-based porous ceramics is used in cooling systems, filter elements and as refractory materials. Silicon nitride-based composites possess enhanced mechanical characteristics: crack resistance, strength, stiffness, etc. As reinforcing inclusions when creating Si_3N_4-based composites the fibers and dispersed particles of various high temperature ceramics are used: aluminum oxide, oxide carbide, titanium oxide, titanium nitride, etc.

This paper reviews the problem of creating composite silicon nitride ceramics using 3D printed technology. Over the last twenty years, several options of additive technological processes for manufacture of the products and blank parts of the products from silicon nitride having complex geometry and different porosity [3, 4, 5, 6, 7, 8, 9, 10, 11, 12]. The process for making the products from silicon nitride by laminated object manufacturing (LOM) method was proposed in papers [3] and [4]. Slurry casting technology in fitment produced by layered modeling method (MoldSDM) was used in paper [5]. Fused Deposition Modelling (FDM) was used in paper [6]. Ceramic preparation from silicon nitride by inkjet printing using modification HP DeskJet 930c printer was proposed in papers [6, 7]. 3D printed technology for silicon nitride high porous ceramic containing more than 70% pores was presented in papers [7, 8, 9, 10, 11]. The products were received by 3D printing method using a standard 3D-printer with water-based solvents. In paper [10], the received material was compared with the analogs synthesized using traditional technology. It was found that the material received by 3D printing had the highest porosity but its mechanical properties were the lowest.

One of the deficiencies in the existing technologies of layered silicon nitride products synthesis can be considered the difficulty in preparation of powder dispersion powder in inkjet direct printing or film containing silicon nitride particles using LOM technology. FDM technology that is depleted of the technological transitions data requires solution of the disposal problem of the grown product in thermoplastic material (polymer or paraffin) of technological binding. This time-consuming process, except that it is not environmentally friendly it often leads to defect of geometrically complex products. One of the technology being also depleted of technological transitions data is layer-by-layer synthesis by Binder Jetting method. General description and principles of reaction sintering technology are presented, for example, in paper [13]. This technology is widely used for 3D printing of the products made of gypsum, mortar sand and even biomaterials. The version of this technology for production of silicon nitride-based ceramics was proposed in recent paper [12]. The problem

of Binder Jetting technology application is high porosity and low mechanical properties in the synthesized products [8, 9, 10, 11, 12] (Figure 1).

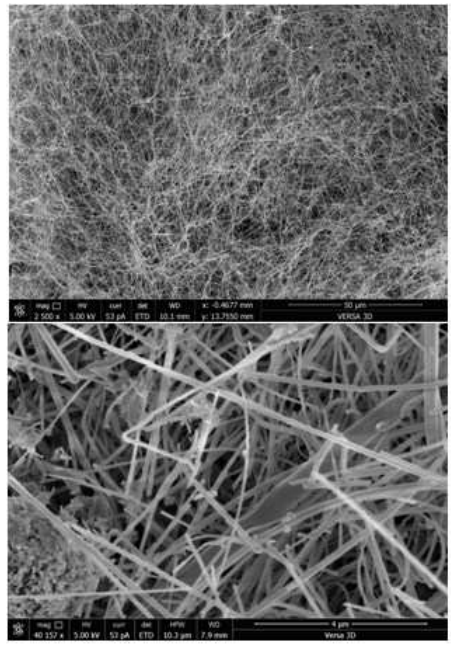

Figure 1: Microstructure of Si_3N_4 porous ceramics received through BinderJet technology.

When using 3D printing technology through Binder Jetting method the products blanks of silicon powder, reinforcing inclusions (for example, silicon carbide particles) and binder [12] shall be produced. Then drying and reaction sintering in the atmosphere of nitrogen shall be performed during which the binder is burned and the silicon nitride structure containing reinforcing inclusions is formed. Due to high content of binder the significant amount of porosity is present in the product blank but the received material comes out to be of low-density. In the process of reaction sintering the significant part of silicon nitride interacting with nitrogen forms high-porous fiber structure (Figure 1). Availability of this structure leads to reduction of mechanical properties of the received products. The use of reinforcing fillers in the form of dispersed inclusions, fibers or filamentary crystals than can be added to the material in 3D printing of the products blanks may be one of the possible solutions to this problem.

In this paper we carry out theoretical modeling of the porous fiber structures cooling processes formed by the fibers of the silicon nitride α-phase and

reinforced spherical particles of silicon carbide. The objective of this research is connected with the need to evaluate the effect of the inclusions on the strength of the material, which is determined to a large extent by the level of the realized residual stresses. It should be noted, that strong enough contact between the fibers and present foreign inclusions is realized in the course of synthesis since, apparently, the fiber material is settled out of the gas phase. Consequently, in the calculations process we anticipate a perfect connection of the fibers together and the fibers with the inclusion without introduction of the additional contacts [14, 15]. When this happens, we must perform calculations on the three-dimensional solid-models without involvement of the core models, as it was done in papers[14, 15]. Thus, the models of the fragments used and the calculation process directly become complicated. This is connected with the need of mandatory use of solid-models for used spherical inclusions and complexity of the contact zones configuration arising between the inclusions and the fibers. Geometry of these zones can impact substantially on the residual stress and therefore requires use of 3D simulation.

2. Modeling Methods

The proposed method includes three main modeling stages. At the first stage, a 3-D model of the representative material fragment with the specified characteristics of porosity volume content, geometry and orientation of fiber, volume content and size of spherical inclusions. Generation of such fiber fragments was described, for example, in papers [16, 17]. At the second stage the model is transferred to the Ansys system where the numerical modeling of stressed and deformation state of the representative fragment in its slow cooling from $1450^{\circ}C$ to room temperature is performed. At the third stage the numerical calculation results are processed and averaged by the volume of the representative fragment to obtain evaluation of the realizing residual stresses.

To generate 3D models Digimat-FE system is used that makes it possible to build 3D models of inhomogeneous materials with complex structure. When creating the representative fragments, fibrous high-porous material is presented in the form of a composite in which the matrix has zero stiffness (voids). The fibers of silicon nitride are simulated in the form of extended cylinders and the particles of silicon carbide – in the form of spheres. The examples of examined representative fragments are shown in Figure 2. Cubic fragments with size of edge in 5 μm were examined containing 10 vol.% of fibers and different number of spherical inclusions with different volume content. To evaluate the effect of

the inclusions and fibers sizes ratio the fragments were examined containing a single inclusion and fragments containing 8 orderly-arranged inclusions (this case corresponds to isotropic-reinforced materials with good dispergation of inclusions [18]). The fibers diameter is known from the experimental data, it makes on average 0.5 μm. The list of all examined structures and their reinforcing parameters are shown in Table 1.

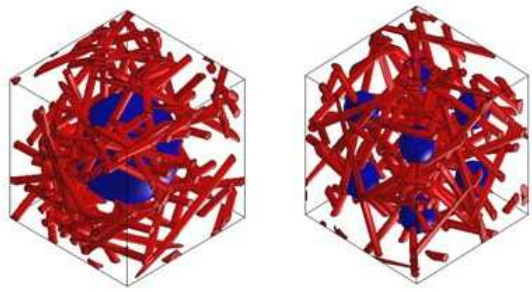

Figure 2: Examples of fibrous structures' representative fragments made of silicon nitride (cylinders red), reinforced by spherical inclusions of silicon carbide (blue spheres), generated in Digimat system. A: fragments containing a single large inclusion, B: fragments containing 8 orderly-arranged fine inclusions.

Table 1: Examined options of fibrous high-porous Si_3N_4-based fiber structures with average diameter of 0.5 μm.

No.	Volume content of inclusions SiC, vol.%	Number of inclusions SiC	Size of inclusions SiC, μm
1	5	1	4,57
2	7.5	1	5,25
3	10	1	5,75
4	12.5	1	6,2
5	15	1	6,6
6	5	8	2,285
7	7.5	8	2,615
8	10	8	2,88
9	12.5	8	3,1
10	15	8	3,295

Received fragments are transmitted into Ansys system in the form of solid

objects. Then, finite-element partition of the models with tetrahedral elements of the first order is created (Figure 3), the properties of Si3N4 fiber materials and SiC inclusions are set, cooling conditions of the structure is established and calculation is performed. In performed calculations, the materials are assumed to be isotropic, their properties are shown in Table 2. The initial temperature of all elements in the fragment is set to the temperature equal to products fusion temperature of $1450^{\circ}C$. Going forward, quasi-stationary cooling of the fragment to $20^{\circ}C$ is set. Calculation is performed in lineal thermoelasticity task assignment [19, 20, 21]. Accordingly, relation between infinitesimal deformations ε_{ij} and movement u_i is used (comma after the indices corresponds to a partial derivative):

$$\varepsilon_{ij} = (u_{i,j} + u_{j,i})/2.$$

Equations of equilibrium in considered quasi-static task without taking into account the volume force are reduced to zero of divergence from stress tensor:

$$\sigma_{ij,j} = 0.$$

Defining relations are entered using Duhamel-Neumann law for accounting the temperature effects (on repeated indices adding is assumed):

$$\sigma_{ij} = C_{ijkl}\varepsilon_{kl} - \beta_{ij}T,$$

accordingly, for the isotropic materials under examination there's a link between the stresses and the strains through Lame parameters μ, λ, modulus of cubic compressibility $K = \lambda + 2\mu$ and thermal expansion coefficient α:

$$\sigma_{ij} = 2\mu\varepsilon_{ij} + (\lambda\varepsilon_{kk} - \alpha KT)\delta_{ij}.$$

On all external surfaces of the fragment and on free surfaces inside it, the limiting conditions on lack of stress are set:

$$\sigma_{ij}n_j = 0,$$

where n_j means the outer normal components to the surface under examination.

On the contact surfaces between fibers and spherical inclusions the equations of the ideal contact with respect to movements and stresses are carried out:

$$(\sigma_{ij}n_j)_{fibers} = (\sigma_{ij}n_j)_{particles},$$
$$(u_i)_{fibers} = (u_i)_{particles}.$$

Displacements and rotations of geometry elements as a rigid body, are eliminated through automatic means of Ansys system.

Table 2: Properties of the materials used in calculations

	Si_3N_4 Fibers	SiC Particles
Young's Modulus, hPa	300	410
Poisson's Ratio	0.26	0.14
Thermal Expansion Coefficient, C^{-1} 10^{-6}	3.2	4.1

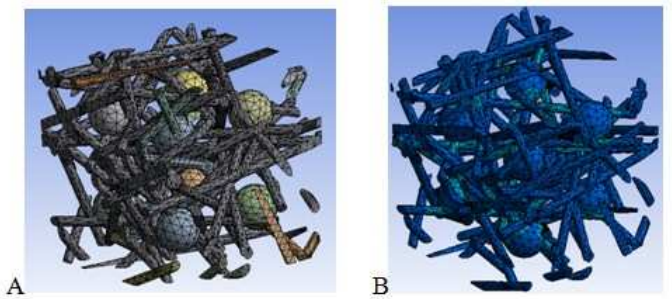

Figure 3: The example of a finite element model (A) and the calculation results of residual stress condition (distribution of the maximum principal stresses) (B) in the representative fragment of Si_3N_4-based fibrous high-porous material comprising eight spherical inclusions of silicon carbide with total volume content of 10%.

When considering plastic materials as a result of the calculation it would be interesting to determine the realizing level of the residual stresses intensity in the material structure. However, the material under examination are fragile, thus as a result of the calculation in the elements of the model maximum and minimum principal values of the stress tensor are defined (Figure 3B). In the course of the simulation, we will be interested in the values of the stresses that are realized in the fibers material since it is the very phase that is the weakest one and its properties and residual stress condition determine macroscopic strength of material. Therefore, to quantify the impact of the inclusions on the residual stress condition of the fibers we determine the average value of maximum σ_I and minimum σ_{III} principal stresses at the nodes of the finite element mesh relating to the fibers and find their average value:

$$\bar{\sigma}_I = \frac{1}{N}\sum_{i=1}^{N}(\sigma_I)_i,$$

$$\bar{\sigma}_{III} = \frac{1}{N}\sum_{i=1}^{N}(\sigma_{III})_i.$$

where N means the total number of nodes of a finite element mesh relating to Si_3N_4 fibers, i index means the node number, in which the target values of the stresses were calculated.

We take received $\bar{\sigma}_I$ and $\bar{\sigma}_{III}$ values as the measure of the residual stresses value in the composite material structure under examination. We compare these values to all examined material reinforcement options. According to the results of the comparison, the conclusion is drawn as to the impact of the various reinforcement options of the material on its residual stress condition and subsequently on its strength.

3. Calculation Data

For numerical calculations performed on the realistic representative fragments, the repeatability test of the calculation data was carried out in the article when examining one-type fragments generated statistically through the same initial microstructural parameters. For each type of the structure shown in Table 1, 5 representative fragments were generated, for which the average target value $\bar{\sigma}_I$ and $\bar{\sigma}_{III}$ were determined.

The example of the specific distribution of maximum principal stresses $\bar{\sigma}_I$ in the nodes of the finite element mesh relating to silicon nitride fibers is shown in Figure 4. It illustrates the results for the structure containing 8 inclusions which volume fraction constitutes 10%. It is seen that average value $\bar{\sigma}_I$ equals to about 15 MPa. This residual stress value is relatively low compared to the strength of the fibers in alpha-phase of silicon nitride. However, even this stress value can be critical for the materials under examination. We specify as the example that the strength of silicon nitride-based high-porous fibrous ceramics received by 3D printing may equal less than 10 MPa. Thus, the residual stresses must be taken into account when forecasting the structures strength. Figure 4 illustrates that a small number of the nodes very high stresses are realized (over 100 MPa), that connected presumably with the presence of concentrators and insufficiently smooth geometry of the model. Not very many nodes with concentration of stresses are produced and we neglect their impact.

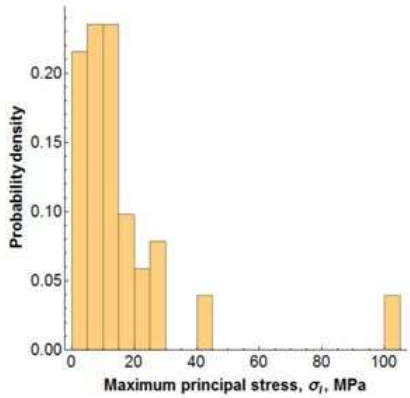

Figure: 4: Specific distribution of maximum principal stress in Si3N4 fibers.

Figure 5 illustrate the calculation data of averaged maximum and minimum principal stresses acting in the fibers, depending on the volume fraction and the number of the filler particles in the representative fragment. In the process of cooling both positive and negative stresses are produced in fibers. This is connected with complex dimensional orientation of the fibers, complexity of their contact with the reinforcing particles and with each other. It is obvious, that with over 15% the residual stress in materials containing fine inclusions can be significant. This, in the first instance, relates to minimum principal strains, maximum level of which constituted -45 MPa (see. Figure 5). Thus, based on the calculation we receive the forecast that silicon nitride fiber structure containing silicon carbide particles after synthetic process can be mainly in compression. At increase of the inclusions volume fraction, in principle, increase in material strength may take place, since stiffness and strength of silicon carbide is much higher compared to the strength and stiffness of fibers. However, established effect can significantly reduce strengthening effect of inclusions. Thus, optimal alternatives the particles' volume content and dispersion can exist apparently.

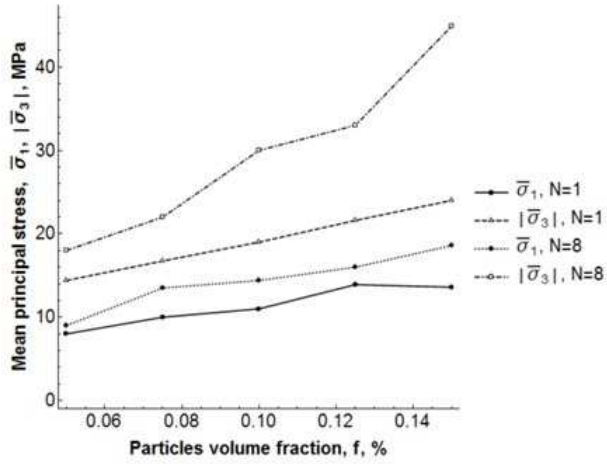

Figure 5: Calculation data of the average maximum and minimum values of the principal residual stresses occurring in silicon nitride fibers in the course of the structures' cooling down that are reinforced with the silicon carbide particles. It illustrates dependence of $\bar{\sigma}_I$ and $|\bar{\sigma}_{III}|$ on the volume and the content and the number of silicon carbide inclusions.

Conclusion

In this paper calculation of the residual stresses produced in silicon nitride-based porous fiber structures, reinforced with the silicon carbide particles has been performed. Calculation is performed within the linear model of thermoelasticity. It is demonstrated, that the volume content and the size of inclusions can have a significant impact on the level of the residual stresses, that are evaluated at the average of maximum and minimum values of the principal stresses produced in the finite element model. It is illustrated that presence of the residual stresses may lead to softening effect at adding of a small volume fraction of fine inclusions.

Obtained results may be useful when selecting the best reinforcement options of the silicon nitride- based ceramic products received by 3D printing and reaction sintering methods or other methods, leading to origination of fibrous porous microstructure of the material.

Acknowledgement

This paper was prepared at the Moscow Aviation Institute financially supported by "Research and Development under Priority Lines of Russian Science and Technology Sector for years of 2014-2020" the Federal Special-Purpose Program, Agreement No. 14.577.21.0171 (unique identifier RFMEFI57715X0171).

References

[1] Z. Krstic, V.D. Krstic, Silicon nitride: the engineering material of the future, *Journal of Materials Science*, **47** (2012), 535-552.

[2] S. Somiya, *Handbook of Advanced Ceramics: Materials, Applications, Processing, and Properties*, Academic Press, USA (2013).

[3] S.J. Rodrigues, R.P. Chartoff, D.A. Klosterman, M. Agarwala, N. Hecht, Solid Freeform Fabrication of Functional Silicon Nitride Ceramics By Laminated Object Manufacturing, *Proceedings of the SFF Symposium*, Texas, (2000), 1-8.

[4] H.-C. Liu, S. Lee, S. Kang, C.F. Edwards, F.B. Prinz, RP of SiN burner arrays via assembly mould SDM, *Rapid Prototyping Journal*, **10** (2004), 239-246.

[5] S. Iyer, J. McIntosh, A. Bandyopadhyay, N. Langrana, A. Safari, S.C. Danforth, P.J. Whalen, Microstructural Characterization and Mechanical Properties of Si_3N_4 Formed by Fused Deposition of Ceramics, *International Journal of Applied Ceramic Technology*, **5** (2008), 127-137.

[6] B. Cappi, E. Özkol, J. Ebert, R. Telle, Direct inkjet printing of Si_3N_4: Characterization of ink, green bodies and microstructure, *Journal of the European Ceramic Society*, **28** (2008), 2625-2628.

[7] B. Cappi, J. Ebert, R. Telle. Rheological properties of aqueous Si_3N_4 and $MoSi_2$ suspensions tailor-made for direct inkjet printing. *Journal of the American Ceramic Society*, **94** (2011), 111-116.

[8] X. Li, L. Zhang, X. Yin, Effect of chemical vapor infiltration of Si_3N_4 on the mechanical and dielectric properties of porous Si_3N_4 ceramic fabricated by a technique combining 3-D printing and pressureless sintering, *Scripta Materialia*, **67** (2012), 380-383.

[9] X. Li, L. Zhang, X. Yin, Microstructure and mechanical properties of three porous Si_3N_4 ceramics fabricated by different techniques. *Materials Science and Engineering*: A, **549** (2012), 43-49.

[10] W. Duan, X. Yin, F. Cao, Y. Jia, Y. Xie, P. Greil, N. Travitzky, Absorption properties of twinned SiC nanowires reinforced Si_3N_4 composites fabricated by 3d-prining, *Materials Letters*, **159** (2015), 257-260.

[11] S. Liu, F. Ye, L. Liu, Q. Liu, Feasibility of preparing of silicon nitride ceramics components by aqueous tape casting in combination with laminated object manufacturing, *Materials and Design*, **66** (2015), 331-335.

[12] L. Rabinskiy et al., Fabrication of porous silicon nitride ceramics using binder jetting technology, *IOP Conference Series: Materials Science and Engineering*, IOP Publishing, **140** (2016), 012023.

[13] I. Gibson, D. Rosen, B. Stucker, Additive Manufacturing Technologies: 3D Printing, Rapid Prototyping, and Direct Digital Manufacturing, Springer (2013).

[14] Q. Liu, Z. Lu, Z. Hu, J. Li, Finite element analysis on tensile behaviour of 3D random fibrous materials: Model description and meso-level approach, *Materials Science and Engineering*, **587** (2013), 36-45. DOI: 10.1016/j.msea.2013.07.087

[15] Z. Lu, Q. Liu, H. Han, D. Zhang, Experiment and modeling on the compressive behaviors for porous silicon nitride ceramics, *Materials Science and Engineering*, **559** (2013), 201-209. DOI: 10.1016/j.msea.2012.08.081

[16] W.W. Sampson, *Modelling Stochastic Fibrous Materials with Mathematica. Chemical Vapor Deposition*, Springer-Verlag London Limited (2009).

[17] S.G. Advani, The Use of Tensors to Describe and Predict Fiber Orientation in Short Fiber Composites. *Journal of Rheology*, **31** (1987), 751-784. DOI: 10.1122/1.549945

[18] S.A. Lurie, D. Volkov-Bogorodskiy, Y. Solyaev, R. Rizahanov, L. Agureev, Multiscale modeling of aluminum-based metal-matrix composites with oxide nanoinclusions, *Computational Materials Science*, **116** (2016), 62-73.

[19] W. Nowacki. *Thermoelasticity*. Elsevier (2013).

[20] S.A. Lurie, E.L. Kuznetsova, E.I. Popova, L.N. Rabinskiy, Improved Gradient Theory of Scale-Depend Ultra-Thin Rods, *Math. Russian Academy of Sciences. Mechanics of Solids*, **2** (2015), 30-43.

[21] S.A. Lurie, S.I. Zhavoronok, P.A. Belov, L.N. Rabinskiy, *Scale Effects in Continuum Mechanics. Materials with Microstructure and Nanostructure*, MAI Press, Moscow (2011).